J. Fluid Mech. (2006), *vol.* 552, *pp.* 299–309.
doi:10.1017/S0022112005008347 Printed in the United Kingdom

Stability of Chapman–Jouguet detonations for a stiffened-gas model of condensed-phase explosives

By MARK SHORT[1], JOHN B. BDZIL[2] AND IANA I. ANGUELOVA[3]

[1]Theoretical and Applied Mechanics, University of Illinois, Urbana, IL 61801, USA

[2]Los Alamos National Laboratory, Los Alamos, NM 87545, USA

[3]Department of Mathematics, University of Illinois, Urbana, IL 61801, USA

(Received 18 May 2005 and in revised form 11 October 2005)

The analysis of the linear stability of a planar Chapman–Jouguet detonation wave is reformulated for an arbitrary caloric (incomplete) equation of state in an attempt to better represent the stability properties of detonations in condensed-phase explosives. Calculations are performed on a 'stiffened-gas' equation of state which allows us to prescribe a finite detonation Mach number while simultaneously allowing for a detonation shock pressure that is substantially larger than the ambient pressure. We show that the effect of increasing the ambient sound speed in the material, for a given detonation speed, has a stabilizing effect on the detonation. We also show that the presence of the slow reaction stage, a feature of detonations in certain types of energetic materials, where the detonation structure is characterized by a fast reaction stage behind the detonation shock followed by a slow reaction stage, tends to have a destabilizing effect.

1. Introduction

A detonation is a form of propagating wave front, consisting of a lead shock sustained by chemical reaction in a following reaction zone, which can occur in gaseous, liquid or solid explosives. The idealized detonation structure in any explosive is a one-dimensional wave front, the Zeldovich–Von Neumann–Döring, or ZND, wave (Fickett & Davis 1979), which in most cases propagates at a minimum speed defined by the presence of a sonic flow point (relative to the detonation wave speed) within the reaction zone, known as the Chapman–Jouguet, or CJ, detonation. However, in gases, this idealized structure is typically unstable, and detonation fronts tend to propagate in a highly unsteady multi-dimensional manner, leading to the formation of spectacular fish-scale patterns on the walls of rectangular shock tubes lined with soot-covered aluminium foil (Fickett & Davis 1979). Several experimental investigations (including schlieren and particle laser-induced fluorescence imaging, e.g. Lee 1984; Kaneshige & Shepherd 1997; Austin, Pintgen & Shepherd 2004) and analysis via direct numerical simulation (e.g. Sharpe 2001; Gamezo *et al.* 2000), have led to a reasonable understanding of the Mach stem, and reflected and lead shock triple-point interactions that underlie the cellular detonation structure in gases.

On the other hand, comparatively little is known about the reaction wave structure in detonating liquid and solid explosives, where the extreme high-pressure environment

($\sim$30–50 GPa) and high wave speeds ($\sim$6–8 km s^{-1}) make experimental diagnostic data collection and imaging difficult. While there is some evidence that detonations in some forms of liquid explosives (such as nitromethane) do exhibit a transverse-wave structure (Fickett & Davis 1979; Engelke & Bdzil 1983), it has not yet been established in all cases whether this is due to an inherent reactive-hydrodynamic instability (as in gases) or due to the effects of explosive confinement (Fickett & Davis 1979). On the other hand, laser-based interferometry measurements of particle velocities in the reaction zone of detonations in pure and commercial-grade liquid nitromethane (Sheffield *et al.* 2002), and in the solid explosives PBX9501 (Gustavsen, Sheffield & Alcon 2000) and PBX9502 (Seitz *et al.* 1989), appear to indicate that the idealized one-dimensional planar structure is stable. For PBX9502, this conclusion is reinforced by velocity against curvature measurements of detonations propagating in cylindrical sticks (Hill, Bdzil & Aslam 2000). However, the rapid time resolution ($\ll$1 ns) required to experimentally resolve the very fine structure of the detonation front in liquid and solid explosives is currently unavailable. Consequently it seems likely at this point in time that advances in our understanding of detonation structure and stability in condensed-phase systems can be made only from mathematical and numerical modelling.

To this end, Short *et al.* (2005) have examined the stability of planar detonations within the context of the idealized condensed-phase model. This reactive-Euler model consists of a constant-γ ideal-gas caloric equation of state having $\gamma = 3$, and assumes a one-step reaction with an algebraic pressure-dependent rate (with a sensitivity measured by an exponent n) and a non-integer reaction order (ν). In the strong shock limit, and with $\nu = 1/2$, the planar CJ detonation is unstable to disturbances within a finite band of wavenumbers for $n > 2.16$, a value which is characteristic of those used to mimic explosives like nitromethane (NM) and PBX9501/2 within the context of the idealized condensed-phase detonation model. Thus the use of this model tends to conflict with the experimental observations that detonations in condensed-phase systems are stable. One of the drawbacks of this model is the use of the ideal-gas caloric equation of state, which, for the typical ratios of detonation-shock pressure to ambient pressure found in condensed-phase systems, results in extremely large detonation Mach number values, since the sound speed in the initial state is proportional to the initial pressure. In practice, for most condensed-phase explosives the characteristic detonation Mach numbers are in the range 2–4. It seems natural, therefore, that we should examine the effect on the location of the neutral stability boundaries found in Short *et al.* (2005) for more realistic equations of state, where the ambient material sound speed can be specified from experiments at a given pressure.

In the following, the classical detonation linear stability problem is reformulated for a caloric (incomplete) equation of state in which the internal energy is specified as an arbitrary function of pressure, specific volume and reaction progress variable. We assume a one-step reaction as in Short *et al.* (2005), but now with an arbitrary reaction rate law. The extension to multiple reaction steps is trivial, but omitted here for reasons of clarity of the analysis. We then describe the extension of the idealized condensed-phase detonation model to a 'stiffened-gas' equation of state (Harlow & Amsden 1971; Menikoff & Plohr 1989; Davis 1997), under which the stability of detonations with finite Mach numbers and large ratios of the post- to pre-shock pressures, found in explosives such as NM and PBX9501/2, can be better modelled. Subsequently, we describe the transition in the location of the one- and two-dimensional neutral stabilities that occurs as the detonation Mach number is systematically decreased from infinite values (Short *et al.* 2005) to finite values, within

the stiffened-gas equation of state model. The linear stability of a detonation for a non-ideal equation of state based on that described in Wescott, Stewart & Davis (2004) has also been examined by Kasimov *et al.* (2003) and Kasimov (2004), including one-step pseudo-reaction models for NM and PBX9502 similar to those used in the current paper, and where, for CJ detonations, the linear spectra are derived in the limit where the detonation overdrive approaches unity, rather than specifically for the CJ case. The current formulation, particularly that of the normal mode eigenfunction boundedness condition required to calculate the linear stability spectra, is for unspecified functional forms for the equation of state and the reaction rate law, and applies specifically at the CJ detonation speed.

A second question is also addressed in the current paper. It is apparent that detonations in liquid nitromethane and PBX9502 are characterized by reaction zones with dual length scales. These multi-length-scale detonations probably occur due to a change in reaction mechanisms within the reaction zone, where one set of explosive components is consumed rapidly behind the detonation shock, and then a second set of components is consumed over a longer time scale (Sheffield *et al.* 2002). For example, detonation particle velocity histories in nitromethane (Sheffield *et al.* 2002) indicate that 70–75 % of the reaction occurs within 10 ns of the passage of the shock, while the latter 25–30 % of the reaction occurs over a time scale of around 50 ns. Similarly in PBX9502 (Seitz *et al.* 1989), 85 % of the reaction occurs within 25 ns of the passage of the detonation shock, while the latter 15 % occurs over 300 ns. Particle velocity histories in PBX9501 (Gustavsen *et al.* 2000) indicate a single-length-scale reaction zone. We address how the presence of a slow reaction stage, characteristic of detonations in NM and PBX9502, affects the location of the detonation stability boundaries.

2. Model

2.1. *Equations*

The non-dimensional equations of motion coupled with an equation for species conservation for the single-step reaction $\mathscr{F}(\text{fuel}) \rightarrow \mathscr{P}(\text{product})$ are given by

$$\frac{\mathrm{D}\Lambda}{\mathrm{D}t} - \Lambda(\nabla^l \cdot \boldsymbol{u}^l) = 0, \quad \frac{\mathrm{D}\boldsymbol{u}^l}{\mathrm{D}t} = -\Lambda \nabla^l p, \quad \frac{\mathrm{D}e}{\mathrm{D}t} = -p\Lambda(\nabla^l \cdot \boldsymbol{u}^l), \quad \frac{\mathrm{D}\beta}{\mathrm{D}t} = r, \qquad (2.1a, b, c, d)$$

for specific volume Λ, pressure p, specific internal energy e, laboratory-frame velocity $\boldsymbol{u}^l = (u^l, v^l)$ and reaction progress variable β, where $\beta = 1$ represents unreacted fuel, and $\beta = 0$ is fully depleted fuel. At this stage we adopt the general incomplete equation of state and reaction rate forms,

$$e = e(p, \Lambda, \beta), \quad r = r(p, \Lambda, \beta). \qquad (2.2a, b)$$

The (chemically) frozen sound speed c is related to (2.2a) via

$$c^2 = \Lambda^2(p + e_{,\Lambda})/e_{,p}. \qquad (2.3)$$

Equations (2.1)–(2.3) have been non-dimensionalized such that $\Lambda = \tilde{\Lambda}/\tilde{\Lambda}_0$, $\boldsymbol{u}^l = \tilde{\boldsymbol{u}}^l/\widetilde{D}$, $p = \tilde{\Lambda}_0 \tilde{p}/\widetilde{D}^2$, $\boldsymbol{x}^l = \tilde{\boldsymbol{x}}^l/\tilde{l}$, $t = \widetilde{D}\tilde{t}/\tilde{l}$, $e = \tilde{e}/\widetilde{D}^2$, $c^2 = \tilde{c}^2/\widetilde{D}^2$, where $\widetilde{\Lambda}_0$ is the upstream (ambient) specific volume and $\widetilde{D}$ is the dimensional (CJ) planar steady detonation velocity. The length scale $\tilde{l}$ is set below.

3. Travelling wave solutions

For thermodynamically consistent forms of (2.2a), the above model supports a one-dimensional steady travelling wave solution consisting of a lead shock followed by a region of chemical reaction (the ZND structure). Issues of thermodynamic consistency for arbitrary equations equations of state relevant to compressible inviscid flows have been extensively discussed by Menikoff & Plohr (1989). In a reference frame attached to the wave, $x = x^l - t$, where $x = 0$ is set by the location of the shock front, the thermodynamic and mechanical states in the steady wave for a general caloric equation of state are connected by the conditions

$$\Lambda = -u, \quad p = u + 1 + p_0, \quad e + p\Lambda + u^2/2 = e_0 + p_0 + 1/2, \tag{3.1a, b, c}$$

where $p_0 = \tilde{\Lambda}_0 \tilde{p}_0 / \widetilde{D}^2$ ($\tilde{p}_0$ is the dimensional unshocked material pressure), $e_0 = \tilde{e}_0 / \widetilde{D}^2$ is the ambient internal energy, and $u = u^l - 1$. Relations (3.1a, b) define the Rayleigh line variation, which holds regardless of the form of (2.2a), while (3.1c) defines the Hugoniot curves for any degree of reaction, which do depend on the form of (2.2a). The spatial structure of the ZND wave can be determined through the Master equation relation,

$$u_{,x} = -\frac{u e_{,\beta}}{\eta e_{,p}} r, \quad \eta = u^2 - c^2, \tag{3.2}$$

which depends on the form of both e and r. This equation is obtained by substituting (2.2a) in the shock-attached steady version of (2.1c), and using (2.3) and (3.1a, b, c) to eliminate p and Λ. Here, η is a sonic parameter. The structure of the CJ wave, the slowest of all possible steady wave solutions, is defined by the appearance of a sonic point relative to the detonation wave speed at a point of either incomplete or complete reaction. For general forms of (2.2a, b) this may be determined as follows (Davis 1997). If $\widetilde{D}_{CJ}$, $\tilde{p}_0$ and $\tilde{e}_0$ are known initially, where $\widetilde{D}_{CJ}$ is the CJ speed, (3.1a, b, c) can be solved to determine the immediate post-shock state at which no reaction has occurred. Subsequently, (3.2) can be integrated from the shock ($x = 0$) into the region $x < 0$. A single value of the heat of reaction $\tilde{q}$ will define a solution trajectory which passes through the critical point (where η and r vanish simultaneously), and it is this trajectory which defines the spatial structure of the CJ wave. Note that if the sonic point appears at the end of the reaction zone, then (3.1a, b, c) can be used to determine $\tilde{q}$ algebraically, otherwise $\tilde{q}$ must be determined iteratively by successive integrations of (3.2). If $\tilde{q}$, $\tilde{p}_0$ and $\tilde{e}_0$ are known initially, a similar procedure can be used to determine $\widetilde{D}_{CJ}$.

4. Linear analysis

4.1. *Perturbation equations*

The equations governing small (linear) perturbations to the steady travelling wave identified in § 3 are constructed as follows. We transform to a new spatial coordinate system $x = x^l - t - \Psi(y, t)$, $y^l = y$, where $x^l = t + \Psi(y^l, t)$ is the shock locus in the laboratory frame, which now becomes $x = 0$. We seek a normal mode decomposition,

$$\Psi = \Psi_0 \exp(\alpha t + \mathrm{i}ky), \quad z = z^* + \Psi_0 z'(x) \exp(\alpha t + \mathrm{i}ky), \tag{4.1}$$

for the growth rate/frequency eigenvalue α and wavenumber k, where $z = (\Lambda,\ u,\ v,\ p,\ \beta)^{\mathrm{T}}$ represents the vector of dependent variables, the superscript* refers to the underlying steady wave solution, the primed quantities indicate the spatially (x) dependent eigenfunctions and $\Psi_0 \ll 1$. The system of equations that

governs the linear stability of a detonation with the general equation of state and reaction rate law (2.2*a*, *b*) is then determined to be

$$\eta^* u^* \boldsymbol{z}'_{,x} + \boldsymbol{A}^* \boldsymbol{z}' + \boldsymbol{a}^* = 0, \tag{4.2}$$

where the matrix $\boldsymbol{A}^*$ is defined in terms of steady-state quantities as

$$\boldsymbol{A}^* = \begin{pmatrix} \alpha\eta + u_{,x}(c^2 - 2u^2) - u^2 a_\Lambda & -\alpha u^2 + u_{,x}(c^2 - 3u^2) \\ u^2(u_{,x} + a_\Lambda) & \alpha u^2 + 2u^2 u_{,x} \\ 0 & 0 \\ c^2 u_{,x} + u^2 a_\Lambda & \alpha c^2 + u_{,x}(c^2 + u^2) \\ -\eta r_{,\Lambda} & \eta\beta_{,x} \end{pmatrix}$$

$$\begin{pmatrix} \mathrm{i}ku^3 & -u^2(\alpha + a_p) & -u^2 a_\beta \\ -\mathrm{i}uc^2 k & u^2(\alpha + a_p) & u^2 a_\beta \\ \alpha\eta & -iku\eta & 0 \\ -\mathrm{i}uc^2 k & u^2(\alpha + a_p) & u^2 a_\beta \\ 0 & -\eta r_{,p} & \eta(\alpha - r_{,\beta}) \end{pmatrix}^*, \tag{4.3}$$

where

$$\left.\begin{aligned} a_p &= (uu_{,x}(e_{,pp} - 1 - e_{,\Lambda p}) + e_{,\beta} r_{,p} + e_{,\beta p} r)/e_{,p}, \\ a_\Lambda &= (uu_{,x}(e_{,p\Lambda} + c^2 e_{,p}/u^3 - e_{,\Lambda\Lambda}) + e_{,\beta} r_{,\Lambda} + e_{,\beta\Lambda} r)/e_{,p}, \\ a_\beta &= (uu_{,x}(e_{,p\beta} - e_{,\Lambda\beta}) + e_{,\beta} r_{,\beta} + r e_{,\beta\beta})/e_{,p}. \end{aligned}\right\} \tag{4.4}$$

The vector $\boldsymbol{a}^*$ is

$$\boldsymbol{a}^* = [\alpha u_{,x}(3u^2 - c^2),\ -2\alpha u^2 u_{,x},\ \mathrm{i}k\eta u u_{,x},\ -\alpha u_{,x}(c^2 + u^2),\ -\alpha\eta\beta_{,x}]^{*\mathrm{T}}. \tag{4.5}$$

4.2. *Shock relations*

The general conservation relations across the detonation shock surface $F(\boldsymbol{x}^l, t) = 0$, are

$$[\beta] = [m] = 0, \quad [m\boldsymbol{u}^l + p\boldsymbol{n}^l] = 0, \quad \left[m\left(e + \tfrac{1}{2}\boldsymbol{u}^l \cdot \boldsymbol{u}^l\right) + p(\boldsymbol{u}^l \cdot \boldsymbol{n}^l)\right] = 0, \tag{4.6}$$

where $m = \rho(\boldsymbol{u}^l - \boldsymbol{V}^l) \cdot \boldsymbol{n}^l$, for shock normal $\boldsymbol{n}^l = \nabla^l F/|\nabla^l F|$ and normal shock velocity $\boldsymbol{V}^l \cdot \boldsymbol{n}^l = -F_{,t}/|\nabla^l F|$. Conditions (4.6) may be linearized, and the perturbation eigenfunctions $\boldsymbol{z}'$ shown to satisfy the shock relations

$$u' = a_u \alpha,\ \ p' = (a_u + 1 + u)\alpha,\ \ v' = -(1 + u)\mathrm{i}k,\ \ \Lambda' = (-a_u + 1 + u)\alpha,\ \ \beta' = 0, \tag{4.7}$$

where

$$a_u = (1 + u)(e_{,p} + e_{,\Lambda} + p_0)/(p + e_{,\Lambda} - e_{,p}) \tag{4.8}$$

and we have dropped the steady-state index notation *. These conditions are valid for the general equation of state (2.2*a*) and are applied at $x = 0$.

4.3. *Compatibility condition*

Steady travelling CJ waves contain a bounding forward-facing sonic characteristic where $\eta = 0$. In principle an asymptotic analysis of (4.2) can be used to obtain the spatial structure of the five independent homogeneous modes and the particular solution of $\boldsymbol{z}'$ as $\eta \uparrow 0$. The presence of the sonic point $\eta = 0$ in the steady CJ wave will generally result in one of the homogeneous modes being spatially unbounded as $\eta \uparrow 0$, whether the point $\eta = 0$ occurs at finite spatial locations or as $x \to \infty$ (Short *et al.* 2005). Provided that the functional form of the reaction rate (2.2*b*) does not lead to any additional unbounded $\boldsymbol{z}'$ modes as $\eta \uparrow 0$, the closure condition which

determines α corresponds to the eigenfunction solution for which the single spatially unbounded mode in z' is eliminated as $\eta \uparrow 0$. This issue has been analysed extensively in Short *et al.* (2005). Under these conditions, the boundedness closure condition can also be derived as follows. Without approximation, any forward travelling plane wave in the x-direction in the shock frame is described by

$$\mathrm{L}_{u+c}p + \frac{c}{\Lambda}\mathrm{L}_{u+c}u = \Psi_{,t}\left(p_{,x} + \frac{c}{\Lambda}u_{,x}\right) - \frac{cv}{\Lambda}\mathrm{L}_y u - vL_y p - \frac{c^2}{\Lambda}\mathrm{L}_y v - \frac{E_{,\beta}r,}{E_{,p}} \tag{4.9}$$

where $\mathrm{L}_{u+c} = \partial_t + (u+c)\partial_x$ and $\mathrm{L}_y = \partial_y - \Psi_{,y}\partial_x$. When (4.9) is linearized about the steady wave in normal mode form (4.1), the operator L_{u+c} will generate the differential terms $(u+c)[p, u]'_{,x}$, which as $\eta \uparrow 0$, and under the conditions described above, will be the source of the single unbounded solution (no sources of singular behaviour will be present in the backward or particle characteristic directions). For bounded solutions we thus require $(u+c)[p, u]'_{,x} = 0$ when $\eta = 0$, whereupon we derive the compatibility (boundedness) condition

$$p' + u' - \mathrm{i}k\alpha^{-1}uv' + 2u_{,x}\alpha^{-1}(u'-\alpha) + b_p p' + b_\lambda \Lambda' + b_\beta \beta' = 0 \tag{4.10}$$

where

$$\left.\begin{aligned} b_p &= (-uu_{,x}(1 - e_{,pp} + e_{,\Lambda p})/e_{,p} + e_{,\beta}r_{,p}/e_{,p} + e_{,\beta p}r/e_{,p} - e_{,pp}e_{,\beta}r/e_{,p}^2)/\alpha, \\ b_\Lambda &= (-uu_{,x}(e_{,\Lambda\Lambda} - e_{,p\Lambda} - 2e_{,p}c^2/u^3)/e_{,p} + e_{,\beta}r_{,\Lambda}/e_{,p} + e_{,\beta\Lambda}r/e_{,p} - e_{,p\Lambda}e_{,\beta}r/e_{,p}^2)/\alpha, \\ b_\beta &= (-uu_{,x}(e_{,\Lambda\beta} - e_{,p\beta})/e_{,p} + e_{,\beta}r_{,\beta}/e_{,p} + e_{,\beta\beta}r/e_{,p} - e_{,p\beta}e_{,\beta}r/e_{,p}^2)/\alpha. \end{aligned}\right\} \tag{4.11}$$

Equation (4.10) is applied at the point in the steady wave where $\eta = 0$. It again applies for general forms of (2.2a, b), and also regardless of whether $\eta = 0$ occurs at a point of incomplete reaction or at the point of complete reaction. Also, depending on the form of (2.2a, b) not all the terms in (4.10) will be important at leading order as $\eta \uparrow 0$. Note that there are certain situations where (4.10) will not ensure bounded solutions, and these are related to specific singular forms of reaction rate (Short *et al.* 2005) that are not considered here.

5. Stiffened-gas equation of state and reaction rate law

As discussed above, one of the drawbacks of the idealized condensed-phase detonation model (Short *et al.* 2005) is that when the detonation shock pressure $p_s \gg p_0$, as occurs in condensed-phase explosives, the associated detonation Mach number is large. In practice, while $p_s \gg p_0$, the detonation Mach numbers are typically in the range 2–4 in condensed-phase explosives due to the large ambient sound speed of the explosive. This limitation can be overcome by employing a more complex choice of incomplete equation of state $p = p(e, \Lambda)$ that will allow $p_s \gg p_0$ with finite detonation Mach numbers. The simplest such system is the 'stiffened-gas' equation of state (Harlow & Amsden 1971; Menikoff & Plohr 1989; Davis 1997),

$$e - e_0 = \frac{(p+a)\Lambda}{\Gamma_0} - \frac{(p_0+a)\Lambda_0}{\Gamma_0} - \lambda q, \quad a = \delta - (\Gamma_0+1)p_0, \quad \delta = \frac{\tilde{c}_0^2}{\tilde{D}^2}, \quad p_0 = \frac{\tilde{\Lambda}_0\tilde{p}_0}{\tilde{D}^2} \tag{5.1}$$

where $\delta^{-1/2}$ is the detonation Mach number with respect to the ambient sound speed, p_0 is the ratio of the ambient pressure $\tilde{p}_0$ to $\tilde{D}^2/\tilde{\Lambda}_0$, and Γ_0 is the Gruneisen gamma,

	$\tilde{\rho}_0$ (g cm^{-3})	$\tilde{c}_0$ (km s^{-1})	$\widetilde{D}_{CJ}$ (km s^{-1})	δ	p_0
NM	1.125	1.65	6.248	0.070	2.3×10^{-6}
PBX9501	1.844	2.5	8.792	0.081	7.1×10^{-7}
PBX9502	1.895	2.9	7.706	0.142	9.0×10^{-7}

TABLE 1. Characteristic properties of the explosives liquid nitromethane (NM), PBX9501 (95 % HMX (cyclotetramethylenetetranitramine) and 5 % binder by weight) and PBX9502 (95 % TATB (triaminonitrobenzene), 5 % Kel-F 800 by weight). Here $\tilde{\rho}_0$ and $\tilde{c}_0$ are the ambient material density and sound speed, while $\widetilde{D}_{CJ}$ is the characteristic planar Chapman–Jouguet detonation speed. All values are based on those given in Marsh (1980). The values of p_0 are calculated assuming $\tilde{p}_0 = 1$ atm.

which is assumed to be constant. Also, λ is the product mass fraction variable and q $(=\tilde{q}/\widetilde{D}^2)$ is the non-dimensional heat of reaction. The stiffened-gas equation of state may be derived from a linearization of the incomplete equation of state near a reference state (Menikoff & Plohr 1989). It reduces to the traditional form of the Tait equation of state under conditions of isentropic flow (Menikoff & Plohr 1989). The issue of identifying suitable thermodynamically consistent thermal equations of state from an incomplete equation of state such as (5.1) has been discussed by Menikoff & Plohr (1989) and Menikoff (2004). The value of a is in principle chosen to fit the experimentally determined sound speed in the material at a given pressure, where $c^2 = (1+\Gamma_0)\Lambda(p + a/(1+\Gamma_0))$. The values of δ and p_0 for the three condensed-phase explosives NM and PBX9501/02 are listed in table 1 based on their material properties given in Marsh (1980). It can be seen that the contribution to a from p_0 is negligible, while the detonation Mach number $\delta^{-1/2}$ ranges from 3.78 in NM to 2.65 for PBX9502. For most materials of interest, the variation in a is in the range 0.05 to 0.2. The idealized condensed-phase detonation model (Short *et al.* 2005) can be recovered by setting $a = 0$.

As in Short *et al.* (2005) we also assume a one-step reaction, although the generalization to multiple reaction steps is trivial. Rather than working with the product mass fraction variable λ, it proves convenient to transform to the reaction progress variable β, which is typically chosen to facilitate the integration of the linearized system (4.2) near the sonic point, based on the asymptotic structure of the solution to (4.2) near this point (Short *et al.* 2005). For the present, we set

$$\frac{\mathrm{D}\lambda}{\mathrm{D}t} = \bar{K}(1-\lambda)^{\nu}, \quad \beta = (1-\lambda)^{\mu}, \quad \frac{\mathrm{D}\beta}{\mathrm{D}t} = r = -\mu\bar{K}\beta^{(\nu+\mu-1)/\mu}, \tag{5.2}$$

where ν is the reaction order, $\beta = 1$ represents the shock state, and $\beta = 0$ represents the product state. The rate constant $\bar{K} = \bar{K}(p, \Lambda, \beta)$ is chosen to mimic the ZND detonation structure of NM and PBX9501/02 described in § 1 as determined by laser-based interferometry measurements of particle velocities (Sheffield *et al.* 2002; Gustavsen *et al.* 2000; Seitz *et al.* 1989). This is given by the 'ignition & growth' model-based form (Lee & Tarver 1980),

$$\bar{K} = K\left[p^{n_1}(1-\omega) + k_r p^{n_2}(1+\omega)\right]/2, \quad \omega = \mathrm{erf}(-(\beta-\beta_c)/\epsilon), \tag{5.3}$$

where K is a constant, set by choosing $\tilde{l}$ so that $x = -1$ corresponds to $\lambda = 1/2$ in the steady ZND wave. The parameter $k_r(<1)$ establishes the ratio of the rates of the slow to fast reaction stages that occur in detonations in NM and PBX9502 (Sheffield *et al.* 2002; Seitz *et al.* 1989). The parameters n_1 and n_2 are the pressure sensitivities in the

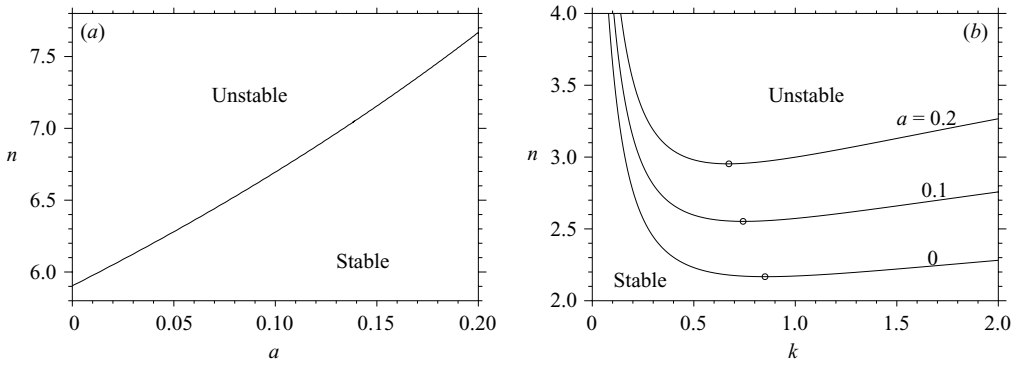

FIGURE 1. (*a*) One-dimensional neutral stability boundaries in the (n, a)-plane when $k_r = 1$. (*b*) Two-dimensional neutral stability boundaries in the (n, k)-plane ($k < 2$) for $a = 0$, $a = 0.1$ and $a = 0.2$ when $k_r = 1$. The circles mark the point of two-dimensional neutral stability in the (n, k)-plane for each a.

fast and slow reaction stages respectively. For $\epsilon \ll 1$, the parameter β_c represents the transition point from the fast to slow reaction stage. When $k_r = 1$ and $n_1 = n_2$ the reaction rate form is identical to that used in Short *et al.* (2005), and is characteristic of the single-length-scale detonation structure found in PBX9501 (Gustavsen *et al.* 2000).

For the stiffened-gas equation of state (5.1) and for a one-step irreversible reaction (5.2), the steady CJ detonation structure can be calculated exactly, and is given by

$$u = -\frac{(1+\Gamma_0)}{(2+\Gamma_0)}(1+\bar{p}_0) + \frac{(1-(1+\Gamma_0)\bar{p}_0)}{2+\Gamma_0}\beta^{1/2\mu}, \quad q = \frac{(1-(1+\Gamma_0)\bar{p}_0)^2}{2\Gamma_0(2+\Gamma_0)}, \tag{5.4}$$

where $\bar{p}_0 = p_0 + a/(1+\Gamma_0)$.

We now present an analysis of the linear stability characteristics of a CJ detonation for the stiffened-gas equation of state (5.1) and reaction rate law (5.2), highlighting the differences with the results found in Short *et al.* (2005). Based on the values given in table 1, in the following we have set $p_0 = 0$, so $a = \delta$, and restricted our range of interest of a to $0 \leqslant a \leqslant 0.2$. We have also set $\nu = \mu = 1/2$ and $\Gamma_0 = 2$. For cases where $k_r = 1$, we use a single pressure exponent $n = n_1 = n_2$, so $\bar{K} = Kp^n$. When $k_r \neq 1$, we set $\epsilon = 0.05$.

6. Results

Figure 1(*a*) shows the variation in the neutral stability boundary that governs one-dimensional ($k = 0$) stability as a varies for $k_r = 1$. For the strong shock limit ($a = 0$), the neutral stability point occurs at $n = 5.904$. Increasing a has a three-fold effect on the CJ wave structure: it reduces the effective heat release q, decreases the shock pressure, while lowering the overall length of the CJ wave. Correspondingly, as a increases, the value of the pressure exponent n at the point of one-dimensional neutral stability increases rapidly. Thus for fixed n, the CJ wave becomes more stable to one-dimensional disturbances as the detonation Mach number decreases. The neutral stability point based on table 1 for NM ($a = 0.07$) occurs at $n = 6.44$, for PBX9501 ($a = 0.081$) at $n = 6.53$ and for PBX9502 ($a = 0.142$) at $n = 7.08$. Figure 1(*b*) shows the neutral stability boundaries that govern stability to two-dimensional disturbances for $k_r = 1$, and three values of a, namely $a = 0$, $a = 0.1$, and $a = 0.2$. Again, increasing

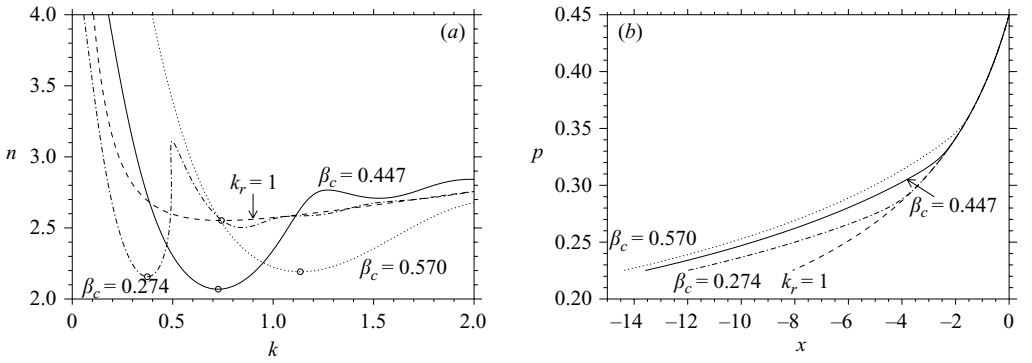

FIGURE 2. (*a*) Two-dimensional neutral stability boundaries for $k < 2$ for $a = 0.1$ and $n = n_1 = n_2$. Shown are the boundaries for $k_r = 1$ and for $k_r = 0.5$ with $\beta_c = 0.274$, 0.447 and 0.570. (*b*) Corresponding CJ wave profiles for $n = 2.5$.

a raises the value of the reaction rate pressure sensitivity exponent n required for instability. Instability when $a = 0$ occurs for $n > 2.168$, when $a = 0.1$ for $n > 2.552$ and when $a = 0.2$ for $n > 2.953$. Thus if one were to assume NM and PBX9501/02 all have the rate form (5.3) with $k_r = 1$ and identical rate pressure sensitivities, $n_1 = n_2$, detonations in PBX9502 would be the most stable.

Figures 2 and 3 concern the effect on stability of a dual-length-scale detonation reaction zone observed in NM and PBX9502, i.e. for $k_r \neq 1$. Figure 2(*a*) shows the two-dimensional neutral stability boundaries found when $a = 0.1$ and $n_1 = n_2 = n$ for $k_r = 1$ and for $k_r = 0.5$ with three different transition points between the fast and slow reaction stages. Figure 2(*b*) shows the corresponding CJ wave pressure profiles for the cases considered in figure 2(*a*) when $n = 2.5$. Due to the second slower reaction stage the length of the CJ wave for $k_r = 0.5$ is greater than that for $k_r = 1$, when the slower reaction stage is absent. As the transition point β_c moves closer to the detonation shock, more of the heat is released in the slow reaction stage, while the overall length of the CJ wave increases. The presence of a slow reaction stage ($k_r < 1$) has a destabilizing effect on the detonation, decreasing the value of n at which instability occurs compared with that when $k_r = 1$. However, there is a non-monotonic behaviour in the value of n above which the CJ wave is unstable as β_c increases. For $\beta_c = 0.274$, the rate pressure exponent above which instability occurs is $n = 2.157$, for $\beta_c = 0.447$, $n = 2.069$, and for $\beta_c = 0.570$, $n = 2.192$. Thus there appears to be a critical value of the ratio of the heat released in the fast reaction stage to that in the slow reaction stage that renders the lowest value of n for instability. Note that there is also a significant variation in the corresponding value of k at the instability onset values of n for the various cases.

Figure 3(*a*) shows the two-dimensional neutral stability boundaries for $a = 0.1$, $\beta_c = 0.447$, when $n_2 = n_1$, $k_r = 0.5$ and $k_r = 0.25$, and when $n_2 = 0.8n_1$, $n_2 = 0.6n_1$ with $k_r = 0.5$. Figure 3(*b*) shows the corresponding CJ wave pressure profiles for the cases considered in figure 3(*a*) when $n = 2.5$. The effect of reducing k_r, keeping the ratio of the heat released in the fast and slow stages constant, is to lower the instability onset value of n. Thus for $n_1 = n_2$, there is a band of instability for $k_r = 0.5$ when $n > 2.069$, and for $k_r = 0.25$ when $n > 1.978$. This trend has been verified for other values of k_r. The final case examined concerns the effect of different rate pressure sensitivities in the fast and slower reaction stages. Figure 3(*a*) also shows the neutral

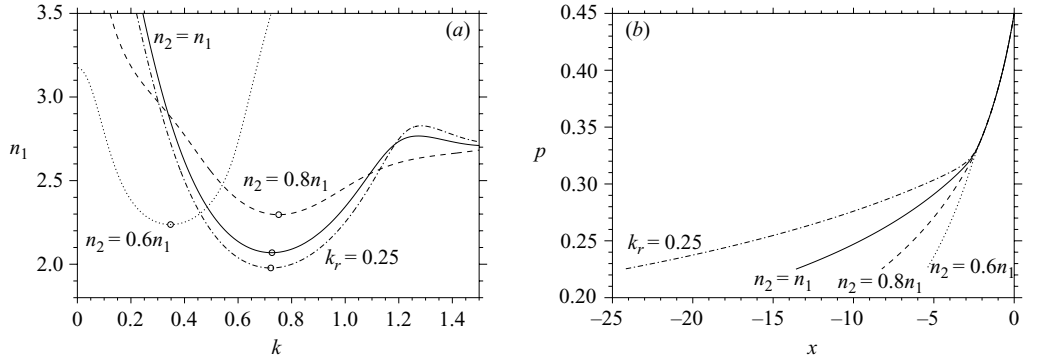

FIGURE 3. (*a*) Two-dimensional neutral stability boundaries for $k < 1.5$, for $a = 0.1$ and $\beta_c = 0.447$. Shown are boundaries for $k_r = 0.5$ and $n_2 = n_1$, $n_2 = 0.8n_1$ and $n_2 = 0.6n_1$ and for $k_r = 0.25$ with $n_2 = n_1$. (*b*) Corresponding CJ wave profiles for $n_1 = 2.5$.

stability boundaries for $n_2 = n_1$, $n_2 = 0.8n_1$, and $n_2 = 0.6n_1$ with $k_r = 0.5$. The decreased sensitivity in the slower reaction stage with k_r fixed diminishes the difference in the rates of the fast and slower reaction stages, and consequently the value of n that determines instability is greater for $n_2 < n_1$ than for $n_2 = n_1$. Again the effect is non-monotonic, since for $n_2 = 0.8n_1$ instability occurs when $n > 2.296$, but for $n_2 = 0.6n_1$ it occurs when $n > 2.237$.

In summary, we have examined the linear stability of a detonation in a condensed-phase material under the assumption of a stiffened-gas equation of state, where the ambient pressure can be ignored relative to the detonation shock pressure when the detonation Mach number is finite. We studied a single-step reaction, with a pressure-sensitive rate that has a single (as occurs in PBX9501) or dual (as occurs in NM or PBX9502) time scale. When the rate pressure sensitivity exponents $n_1 = n_2 = n$, $k_r = 1$, the effect of a decreasing detonation Mach number is to increase the value of n at which instability occurs. For $n_1 = n_2 = n$, $k_r < 1$, the presence of a fast reaction stage followed by a slow reaction stage in the CJ wave tends to decrease the value of n at which instability occurs relative to the value of n for which instability occurs if the second slower reaction were absent. Finally, for cases where $n_2 < n_1$, $k_r < 1$, the value of n_1 for which instability occurs is higher that that when $n_2 = n_1$. In summary, it appears that the detailed underlying CJ detonation wave structures in NM and PBX9501/02 can have a major impact on their stability properties.

REFERENCES

AUSTIN, J. M., PINTGEN, F. & SHEPHERD, J. E. 2004 Reaction zones in highly unstable detonations. *Proc. Combust. Inst.* **30**, 1849–1857.

DAVIS, W. C. 1997 Shock waves; rarefraction waves; equations of state. In *Explosive Effects and Applications* (ed. J. J. Zukas & W. P. Walters). Springer.

FICKETT, W. & DAVIS, W. C. 1979 *Detonation.* University of California Press.

ENGELKE, R. & BDZIL, J. B. 1983 A study of the steady-state reaction-zone structure of a homogeneous & a heterogeneous explosive. *Phys. Fluids* **26**, 1210–1221.

GAMEZO, V. N., VASILEV, A. A., KHOKHLOV, A. M. & ORAN, E. S. 2000 Fine cellular structures produced by marginal detonations. *Proc. Combust. Inst.* **28**, 611–617.

GUSTAVSEN, R. L., SHEFFIELD, S. A. & ALCON, R. R. 2000 Progress in measuring detonation wave profiles in PBX9501. In *Proc. Eleventh Symp. (Intl) on Detonation Office of Naval Research Rep.* ONR 3330000-5, pp. 821–827.

Harlow, F. & Amsden, A. A. 1971 *Fluid Dynamics*. Mongraph LA-4700 (Los Alamos Scientific laboratory, Los Alamos, NM).

Hill, L. G., Bdzil, J. B. & Aslam, T. D. 2002 Front curvature rate stick measurements and detonation shock dynamics calibration for PBX9502 over a wide temperature range. In *Proc. Eleventh Symp. (Intl) on Detonation. Office of Naval Research Rep.* ONR 33300-5, pp. 1029–1037.

Kaneshige, M. & Shepherd, J. E. 1997 Detonation database. *Tech. Rep.* FM97-8, GALCIT, July 1997. See also http://www.galcit.caltech.edu/detn_db/html/.

Kasimov, A. R. 2004 Theory of instability and nonlinear evolution of self-sustained detonation waves. PhD Thesis, University of Illinois At Urbana-Champaign.

Kasimov, A. R. Wescott, B. L. Stewart, D. S. & Yoo, S. 2003 The structure and stability of high-explosive detonation waves. Presented at the *19th Intl Colloquium on the Dynamics and Explosions and Reactive Systems, Hakone, Japan.*

Lee, E. L. & Tarver, C. M. 1980 Phenomenological model of shock initiation in heterogeneous explosives. *Phys. Fluids* **23**, 2362–2372.

Lee, J. H. S. 1984 Dynamic parameters of gaseous detonations. *Annu. Rev. Fluid Mech.* **16**, 311–336.

Marsh, S. P. (Ed). 1980 *LASL Shock Hugoniot Data*. University of California Press, Berkeley.

Menikoff, R. 2004 Empirical equations of state for solids. *Los Alamos National Rep.* LA-UR-04-7353.

Menikoff, R. & Plohr, B. J. 1989 The Riemann problem for fluid flow of real materials. *Rev. Mod. Phys.* **61**, 75–130.

Sharpe, G. J. 2001 Transverse waves in numerical simulations of cellular detonations. *J. Fluid Mech.* **447**, 31–51.

Sheffield, S. A., Engelke, R., Alcon, R. R., Gustavsen, R. L., Robins, D. L., Stahl, D. B., Stacy, H. L. & Whitehead, M. C. 2002 Particle velocity measurements of the reaction zone in nitromethane. In *Proc. Twelfth Symp. (Intl) on Detonation. Office of Naval Research Rep.*

Seitz, W. L., Stacy, H. L., Engelke, R., Tang, P. K. & Wackerle, J. 1989 Detonation reaction zone structure of PBX9502. In *Proc. Ninth Symp. (Intl) on Detonation." Office of Naval Research Rep.* OCNR 113291-7, pp. 657–669.

Short, M., Anguelova, I. I., Aslam, T. D., Bdzil, J. B., Henrick, A. K. & Sharpe, G. J. 2005 Stability of idealized condensed phase detonations. *J. Fluid Mech.* (submitted).

Wescott, B. L., Stewart, D. S. & Davis, W. C. 2004 Calibration of a wide-ranging equation of state and reaction rate for PBX-9502. Presented at the *30th Intl Symp. on Combustion, Chicago, USA*.